

Calculated electron-phonon contributions to phonon linewidths and to the electronic mass enhancement in Pd

F. J. Pinski

Department of Physics, State University of New York at Stony Brook, Stony Brook, New York 11794

W. H. Butler

Metals and Ceramics Division, Oak Ridge National Laboratory, P. O. Box X, Oak Ridge, Tennessee 37830

(Received 13 December 1978)

This paper presents a calculation of the linewidths of phonons in Pd owing to decay into electron-hole pairs. Korringa-Kohn-Rostoker energies and wave functions are used with the rigid-muffin-tin approximation (for the electron-phonon matrix element). The linewidths of the longitudinal $[\zeta 00]$ phonons show a sharp maximum which is in qualitative agreement with the recent experimental observations of Youngblood *et al.* Relatively large linewidths are calculated for a transverse mode (T_1) along the $[110]$ direction, which are in good agreement with the previous experiment of Müller. Both the matrix element and the joint density of states at the Fermi energy contribute to the magnitude of the calculated linewidths. The electron-phonon contribution to the electronic mass enhancement is calculated to be 0.41. This result is used to estimate the contribution due to paramagnetic fluctuations.

I. INTRODUCTION

Palladium is an interesting metal for several reasons. Although it is in the same column of the Periodic Table as nickel and possesses a high magnetic susceptibility,¹ it is not a ferromagnet. Although the electronic density of states at the Fermi energy is large, as is the electronic mass enhancement,²⁻⁴ palladium is not a superconductor. Furthermore, the temperature dependence of the resistivity⁵ and magnetic susceptibility of palladium are anomalous.⁶

The current theoretical model for Pd emphasizes strong Coulomb many-body effects which enhance the Fermi energy electronic mass and the magnetic susceptibility while preventing superconductivity.⁷⁻¹⁰ Unfortunately, this model is not quantitative at present due to experimental and theoretical difficulties. On the theoretical side it is not yet possible to calculate (even approximately) the screened Coulomb matrix elements for a metal like Pd. On the experimental side the precise magnitude of the magnetic Pauli susceptibility enhancement is difficult to determine because of the difficulty of separating the susceptibility into its various components (Pauli, orbital, core diamagnetic, etc.). Similarly it is difficult to identify the Coulombic (or spin-fluctuation) mass enhancement because of the simultaneous presence of the electron-phonon mass enhancement. The work described in this paper is a step in the unraveling of this puzzle. We have calculated the electron-phonon component of the electronic mass enhancement using realistic energy bands and wave functions. Comparison of the electron-phonon

component of the mass enhancement with the total mass enhancement as determined by low-temperature specific-heat or de Haas-van Alphen measurements allows estimation of the Coulombic mass enhancement.

The difficult part of electron-phonon calculations is the choice of matrix elements. We use the rigid-muffin-tin description¹¹⁻¹³ of the electron-phonon coupling, and within this model, this calculation has been done to high precision. However, there is no *a priori* way to judge the accuracy of the rigid-muffin-tin model. Fortunately, several independent experimental checks confirm that this description gives accurate results for Pd. One of the checks is the resistivity which we have calculated using the same electron-phonon matrix elements.¹⁴ A second and more basic check is the phonon linewidth which probes the electron-phonon interaction in great detail.¹⁵ The primary objectives of this paper are to describe our calculation of the electron-phonon contribution to the phonon linewidth, to compare our results with the available experimental data, and to make a tentative estimate of the Coulombic mass enhancement.

II. CALCULATED PHONON LINEWIDTHS

The phonon linewidths reported here were calculated in the same manner as those reported previously for Nb.^{16,17} A Korringa-Kohn-Rostoker (KKR) band-theory program operating in a constant-energy mode was used to generate wave vectors and wave functions for a dense mesh of 676 points on the irreducible $1/48$ th of the Fermi surface. Phase shifts and a Fermi energy density-

of-states analysis for the crystal potential used here have been given previously.⁴ The wave functions and wave vectors were used to calculate the electron-phonon contribution to the phonon linewidth according to Eqs. (1.12) and (1.13) of Ref. 17. As in our previous work, the "rigid-muffin-tin" approximation¹¹⁻¹³ was used to construct the electron-phonon matrix elements.

The calculated linewidths for phonon wave vectors along symmetry directions are shown in Fig. 1. Several interesting features are worthy of note: (i) There is a sharp peak in the longitudinal-mode $[\zeta 0 0]$ linewidth for $\zeta \approx 0.32$. (ii) The $[\zeta 0 0]$ transverse linewidths are quite small. (iii) There are sizable transverse-mode (T_1) linewidths along $[\zeta \zeta 0]$ for $0.3 \lesssim \zeta \lesssim 0.6$. (iv) The longitudinal-mode linewidths increase rapidly with phonon momentum q near $q=0$, especially in the $[\zeta \zeta 0]$ and $[\zeta \zeta \zeta]$ directions.

Feature (i) as predicted by our calculation has recently been confirmed by the inelastic-neutron-scattering measurements of Youngblood *et al.* (Ref. 18, following paper). Features (ii) and (iii) are in good agreement with the measurements of Miiller.¹⁹

(i) To understand the origin of the longitudinal $[\zeta 0 0]$ peak, a subset of the contributing Fermi-surface transitions are shown as the horizontal arrows in Fig. 2. The Fermi surface of Pd consists of four sheets, only three of which are used here.^{2,3,20} The "jungle-gym" sheet is the only important sheet for determining the phonon linewidths. This sheet is an open surface consisting of "arms" or "pipes" which intersect at right angles at the X points. Also shown in Fig. 2 is a Γ -centered sheet of relatively low-mass electrons and an X-centered ellipsoidal hole sheet. The spanning

vectors shown in Fig. 2 connect points on opposite arms of the "jungle gym." Since the arms of the calculated Fermi surface have a very uniform cross section in the (001) plane all three spanning vectors have essentially the same momentum $q \approx [1.68, 0, 0]$, which after reduction by a reciprocal-lattice vector is equivalent to $[0.32, 0, 0]$. The transitions can equally well be viewed as connecting opposing points on the same arm of the jungle gym. Thus the position of the longitudinal $[\zeta 0 0]$ peak is determined by the width of the jungle-gym arms in the (001) plane. The emphasis on the (001) plane is largely a matrix element effect for which we do not have a simple explanation. A similar effect is observed in Nb.¹⁷

Also shown in Fig. 2 is the experimental trace in the (001) plane of the "jungle gym" as determined from de Haas-van Alphen measurements.²⁰ The arms of the jungle gym are somewhat wider and more variable than in our calculation. The experimental width varies from 0.35 to 0.44 in units of $2\pi/a$ so that the peak should be shifted to $\zeta \approx 0.4$, as seen experimentally (see Fig. 2 of Ref. 18). It should be emphasized that this peak is not a simple "nesting" effect but is caused by the matrix elements.

(ii) The calculated linewidths for the $[\zeta 0 0]$ transverse modes are quite small, especially in the vicinity of the longitudinal-mode peak. This feature is in agreement with Miiller's measurements and is due to the fact that the transitions which contribute to the longitudinal peak connect Fermi-surface points which are usually related by reflection in a mirror plane, e.g., (100) plane. For the transverse modes, such transitions have vanishing matrix elements (see Appendix I of Ref. 17).

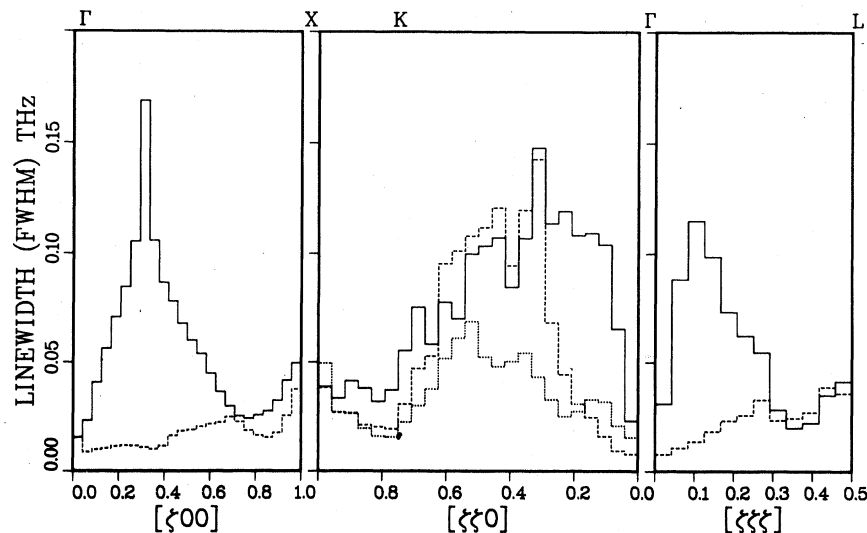


FIG. 1. Calculated linewidths for phonons propagating along symmetry directions. Solid histograms indicate values for the longitudinal modes; the dotted histogram for the [110] direction indicates the T_2 transverse modes.

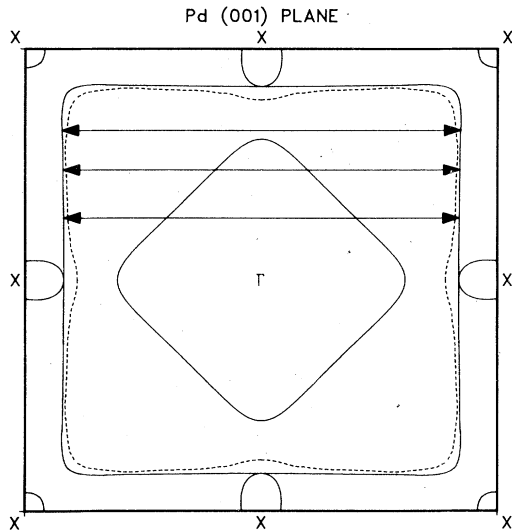


FIG. 2. Intersection of the Fermi surface of Pd with the (001) plane. The solid lines indicate the surface used in this calculation. The dotted lines denote the surface as determined by de Haas-van Alphen experiments (Ref. 20). The arrows are a sample of the main contributions to the linewidth peak in the [100] direction.

(iii) The only appreciable transverse-mode linewidths predicted by our calculations are for the T_1 mode (polarization along $[1\bar{1}0]$ propagating in the $[\zeta\zeta 0]$ direction). Transverse-mode linewidths are generally easier to measure with inelastic neutron scattering due to focusing effects.^{18,21} Our results for these modes are in rather good agreement with the earlier measurements of Miiller¹⁹ as shown in Fig. 3. We have recalculated the experimental linewidths from Miiller's data based on the assumption that the observed width is a convolution of a Gaussian instrumental line shape and a Lorentzian electron-phonon line shape²² rather than two Gaussian line shapes. This correction is significant if the observed and instrumental widths are comparable.

The transitions which contribute to the $[\zeta\zeta 0]$ T_1 linewidth for $\zeta \approx 0.3$ largely lie across the arm of the jungle gym in the (001) plane. For larger ζ they tend not to lie in symmetry planes. Miiller also measured T_1 linewidths along [110] at 296 and 853 K. The structure is less pronounced at higher temperatures. This smearing may be partly due to increased phonon-phonon scattering. But it is difficult to accept this as the entire answer, since the average linewidth does not increase significantly with temperature. Another important factor is the contribution from transitions between states within $\sim \pm 3 k_B T$ of the Fermi surface. Because the jungle-gym velocities are small, $\langle \Delta E / \Delta k \rangle \sim 0.075$ Ry Å, at 853 K, Δk is 0.43 \AA^{-1} which is

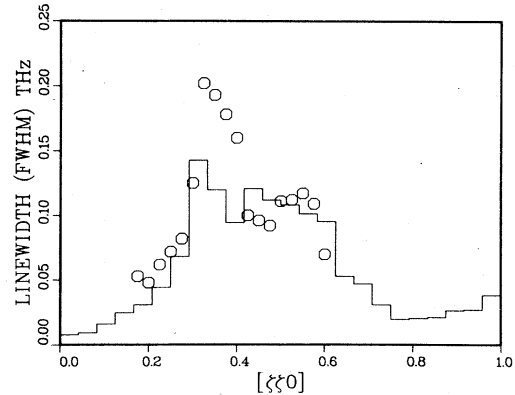


FIG. 3. Linewidths for transverse phonons (T_1) in the [110] direction. Both our calculation (solid histogram) and the experimental results of Miiller (Ref. 19) (circles) are displayed.

25% of the distance between Γ and K .

The large $[\zeta\zeta 0]$ T_1 linewidths coincide with an anomaly in the phonon frequency dispersion. Watson-Yang and Freeman²³ find an enhancement in their "generalized" susceptibility in this region of the Brillouin zone.

(iv) The calculation predicts a rapid increase of the linewidth with ζ at low ζ for the longitudinal modes, especially for the $[\zeta, \zeta, 0]$ and $[\zeta, \zeta, \zeta]$ directions. This strong electron-phonon coupling for low momentum phonons shows up strongly in the calculated spectral functions $\alpha^2 F(\omega)$ and $\alpha^2(+xx)F(\omega)$ (see Ref. 14 for definitions of these quantities). At present there is no experimental confirmation of this strong coupling at low momentum transfer. It seems to arise from the rapid variation of wave-function character with wave vector on the jungle-gym sheet.

III. JOINT FERMI ENERGY DENSITY OF STATES

It was pointed out in Ref. 17 that the structure in the linewidth can be viewed as arising from three sources operating simultaneously. Knowing only the shape of the Fermi surface, the Fermi-surface intersection of two sheets s and s' can be calculated:

$$I_{ss'}(q) = \frac{\Omega_a}{(2\pi)^3} \int_s dS_k \int_{s'} dS_{k'} \delta(k - k' - q), \quad (3.1)$$

where Ω_a is the atomic volume and the integrals are over sheets s and s' of the Fermi surface. $I_{ss'}(q)$ determines the phonon momenta for which these two sheets yield linewidth contributions considering geometry alone. If the Fermi velocities v_k are also known the joint Fermi energy density of states (JFEDOS) can be calculated by

$$J_{ss'}(q) = \frac{\Omega_a}{(2\pi)^3} \int_s \frac{dS_k}{\hbar v_k} \int_{s'} \frac{dS_{k'}}{\hbar v_{k'}} \delta(k - k' - q). \quad (3.2)$$

$J_{ss'}(q)$ is very similar to $I_{ss'}(q)$ but allows for the variation in density of states on the Fermi surface.

Calculated values of $I_{ss'}(q)$ and $J_{ss'}(q)$ are shown in Fig. 4 for s and s' both being the jungle-gym sheet. The total JFEDOS is dominated by this contribution. The significant feature of Fig. 4 is how greatly it differs from Fig. 1. The longitudinal $[\zeta 00]$ linewidth peak, which originates from intrasheet jungle-gym transitions largely in the (001) plane, is a small feature in the JFEDOS. The only difference between the JFEDOS of Fig. 4 and the linewidths of Fig. 1 is the inclusion of the electron-phonon matrix elements in the linewidths. Thus the matrix elements are crucial to understanding the mode and momentum dependence of the electron-phonon interaction.

IV. ELECTRON-PHONON COUPLING CONSTANT AND SPECTRAL FUNCTION

The spectral function $\alpha^2 F(\omega)$ can be calculated directly from linewidths using Eq. (1.18) of Ref. 17. A Born-von Kármán interpolation of the neutron scattering data by Müller and Brockhouse²⁴ was used to determine the phonon dispersion and polarization vectors. The spectral function has been presented previously^{14,15} and is characterized by large values of α^2 at low ω . This effect is particularly noticeable when $\alpha^2 F(\omega)$ for Pd is contrasted with $\alpha^2 F(\omega)$ calculated for Nb^{17,26} or for Mo,²⁵ and it arises from the large linewidths of the longitudinal modes for low phonon momentum.

The value $\lambda = 0.41$ for the electron-phonon cou-

pling constant or mass enhancement is calculated from the spectral function by

$$\lambda = 2 \int \alpha^2 F(\omega) \omega^{-1} d\omega. \quad (4.1)$$

Other quantities calculated from the spectral function are²⁷

$$\begin{aligned} \omega_{\log} &= \exp\left(\frac{\int \alpha^2 F(\omega) \omega^{-1} \ln \omega d\omega}{\int \alpha^2 F(\omega) \omega^{-1} d\omega}\right) = 2.71 \text{ THz}, \\ \langle \omega \rangle &= \int \alpha^2 F(\omega) d\omega / \int \alpha^2 F(\omega) \omega^{-1} d\omega = 3.135 \text{ THz}, \\ \langle \omega^2 \rangle &= \int \alpha^2 F(\omega) \omega d\omega / \int \alpha^2 F(\omega) \omega^{-1} d\omega \\ &= 11.95 \text{ (THz)}^2. \end{aligned} \quad (4.2)$$

If the calculated λ and ω_{\log} , and an assumed μ^* of 0.13 are used in the Allen-Dynes modification of McMillan's formula for the superconducting transition temperature,^{28,29} the result is 0.3 K.

V. ANISOTROPY OF THE MASS ENHANCEMENT

The mass enhancement λ_k due to the electron-phonon interaction varies somewhat with k on the Fermi surface. The mass enhancement averaged over the entire Fermi surface $\lambda = \langle \lambda_k \rangle$ is seen in specific-heat measurements. However, in the de Haas-van Alphen experiments, the measured mass enhancement has been averaged only over the appropriate orbit. Naturally these mass enhancements depend on the specific orbit. Variations of the mass enhancement are often larger between different sheets than on a single sheet. This can be understood in terms of the similar character of the wave functions on an individual sheet. For

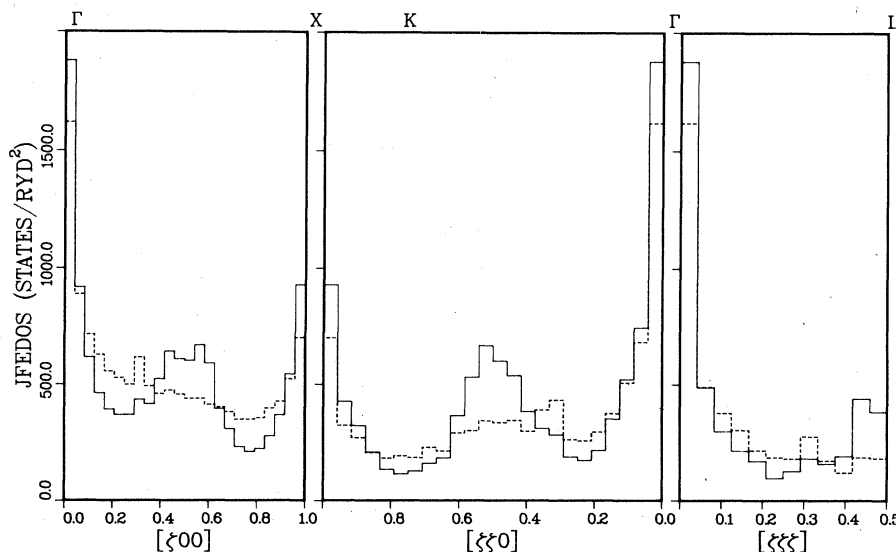


FIG. 4. Joint Fermi energy density of states $J_{ss'}$ (solid histogram) and Fermi-surface intersection $I_{ss'}$ (dashed histogram). The sheet designated by both s and s' is the "jungle gym." The Fermi-surface intersection has been divided by the square of the average Fermi velocity.

this reason, the mass enhancement averaged only over a specific sheet may give insight into these experiments. For a sheet s of the Fermi surface, λ averaged only on that sheet is denoted by λ_s and is given by Eq. (3.5) in Ref. 17 (see Table I). For Pd, approximately 90% of each λ_s is a result of scattering into an electronic state on the "jungle gym", the reason being that 90% of the total density of states resides on this sheet. Our values of λ_s are very similar, varying from 0.381 on the ellipsoids to 0.415 on the jungle gym.

VI. DISCUSSION AND CONCLUSIONS

The generally good agreement between our calculations of the electron-phonon interaction and experimental measurements of resistivity and phonon linewidth substantiates our calculated value of the electron-phonon mass enhancement in Pd (0.41). The *total* mass enhancement can be obtained (one hopes) by comparing specific-heat measurements with band-theory values for the Fermi energy density of states. Fortunately, most band calculations²⁻⁴ seem to agree that the unenhanced Fermi energy density of states for Pd is approximately 16 states (Ry atom spin), while the enhanced density of states obtained from specific-heat measurements³⁰ is 27.5 states/(Ry atom spin). The total enhancement is $\lambda_T = 0.72$. Subtracting 0.41 for the electron-phonon component leaves a "spin-fluctuation" enhancement of $\lambda_{SF} = 0.31$. This value is quite close to the value 0.35 assumed by Fay and Appel¹⁰ in estimating the "*p*-wave" superconducting transition temperature.

Palladium seems to be performing a delicate balancing act. Presumably if spin-fluctuation effects were slightly stronger it would be either a ferromagnet or a paramagnon coupled "*p*-wave" superconductor, and if electron-phonon effects were slightly stronger it would be an "*s*-wave" superconductor. It is, however, none of the above

TABLE I. Anisotropy of the electron-phonon coupling constant λ_s . The three sheets of the Fermi surface are shown in Fig. 2. The density of states for each sheet, N_s , is also displayed.

s	Sheet	λ_s	N_s (Ry spin) ⁻¹
1	Jungle gym	0.415	13.8
2	Γ -centered sheet	0.405	1.3
3	X-centered ellipsoids	0.381	0.4
All sheets		0.414	15.5

for temperatures as low as 1.7 mK.³¹ The absence of *s*-wave superconductivity seems to be roughly consistent with our results for λ_{ep} and λ_{SF} since Gladstone *et al.*⁹ have proposed the following criterion for a vanishing T_c :

$$\lambda_{\text{eff}} = \lambda_{ep} - \lambda_{SF} - \mu^* - 0.62\lambda_{ep}\mu^* \rightarrow 0. \quad (6.1)$$

Using the above value for λ_{ep} , λ_{SF} , and μ^* , we obtain $\lambda_{\text{eff}} = -0.06$.

Our results reported in Ref. 14 for the "*p*-wave" coupling constant were similarly pessimistic. More detailed discussions of both the "*p*-wave" coupling constants and the transport coefficients of Pd will be given in future publications.

ACKNOWLEDGMENTS

We thank B. L. Gyorffy, R. Youngblood, Y. Noda, and G. Shirane for their interest in these calculations. We express a special thanks to P. B. Allen for many useful conversations. One of us (F.J.P.) acknowledges support by NSF Grant No. DMR 76-82946. W. H. B. acknowledges support by the Materials Science Division, U. S. Department of Energy under Contract No. W-7405-eng-26 with the Union Carbide Corporation.

¹S. Foner, R. Doelo, and E. J. McNiff, Jr., *J. Appl. Phys.* **39**, 551 (1968).

²O. K. Anderson, *Phys. Rev. B* **2**, 884 (1970).

³F. M. Mueller, A. J. Freeman, J. O. Dimmock, and A. M. Furdyna, *Phys. Rev. B* **1**, 4617 (1970).

⁴W. H. Butler, *Phys. Rev. B* **15**, 5267 (1977).

⁵M. J. Laubitz and T. Matsumura, *Can. J. Phys.* **50**, 196 (1972).

⁶A. J. Manuel and J. M. P. St. Quinton, *Proc. R. Soc. A* **273**, 412 (1963).

⁷N. F. Berk and J. R. Schrieffer, *Phys. Rev. Lett.* **17**, 433 (1966).

⁸S. Doniach and S. Engelsberg, *Phys. Rev. Lett.* **17**, 750 (1966).

⁹G. Gladstone, M. A. Jensen, and J. R. Schrieffer, in *Superconductivity*, edited by R. D. Parks (Marcel Dekker, New York, 1969), Vol. 2, p. 665.

¹⁰D. Fay and J. Appel, *Phys. Rev. B* **16**, 2325 (1977).

¹¹S. K. Sinha, *Phys. Rev.* **169**, 477 (1968).

¹²G. D. Gaspari and B. L. Gyorffy, *Phys. Rev. Lett.* **28**, 801 (1972); W. H. Butler, J. J. Olson, J. S. Faulkner, and B. L. Gyorffy, *Phys. Rev. B* **14**, 3823 (1976).

¹³W. John, *J. Phys. F* **3**, L231 (1973).

¹⁴F. J. Pinski, P. B. Allen, and W. H. Butler, *Phys. Rev. Lett.* **41**, 431 (1978).

¹⁵P. B. Allen, *Phys. Rev. B* **6**, 2577 (1972).

¹⁶W. H. Butler, H. G. Smith, and N. Wakabayashi, *Phys. Rev. Lett.* **39**, 1004 (1977).

- ¹⁷W. H. Butler, F. J. Pinski, and P. B. Allen, *Phys. Rev. B* **19**, 3708 (1979).
- ¹⁸R. Youngblood, Y. Noda, and G. Shirane, *Phys. Rev. B* **19**, 3708 (1979) (following present paper).
- ¹⁹A. P. Miiller, *Can. J. Phys.* **53**, 2491 (1975).
- ²⁰G. W. Crabtree, D. H. Dye, and D. P. Karim (to be published).
- ²¹S. M. Shapiro, G. Shirane, and J. D. Axe, *Phys. Rev. B* **12**, 4899 (1975).
- ²²D. W. Posner, *Aust. J. Phys.* **12**, 184 (1959).
- ²³T. J. Watson-Yang and A. J. Freeman (to be published).
- ²⁴A. P. Miiller and B. N. Brockhouse, *Can. J. Phys.* **49**, 704 (1971).
- ²⁵F. J. Pinski, P. B. Allen, and W. H. Butler, *J. Phys. (Paris)* **39**, C6-472 (1978).
- ²⁶B. M. Harmon and S. K. Sinha, *Phys. Rev.* **16**, 3919 (1977).
- ²⁷The value of ω_{\log} given on page 433 of Ref. 14 is incorrect. It should be 2.71 THz or 130 K. The correct number was used to calculate T_c .
- ²⁸P. B. Allen and R. C. Dynes, *Phys. Rev. B* **12**, 905 (1975).
- ²⁹W. L. McMillan, *Phys. Rev.* **167**, 331 (1968).
- ³⁰F. E. Hoare and B. Yates, *Proc. R. Soc. A* **240**, 42 (1975); G. Chouteau, R. Fourneaux, K. Gobrecht, and R. Tournier, *Phys. Rev. Lett.* **20**, 193 (1968).
- ³¹R. A. Webb, J. B. Ketterson, W. P. Halperin, J. J. Vuillemin, and N. B. Sandesara, *J. Low Temp. Phys.* **32**, 659 (1978).